Antarctic Science 24(4), 342–352 (2012) © Antarctic Science Ltd 2012 doi:10.1017/S0954102012000041

Bound water freezing in Antarctic *Umbilicaria aprina* from Schirmacher Oasis

H. HARAŃCZYK[1], P. NOWAK[1], M. BACIOR[1], M. LISOWSKA[2], M. MARZEC[1], M. FLOREK[1] and M.A. OLECH[2]

[1]*Institute of Physics, Jagiellonian University, ul. Reymonta 4, 30-059 Cracow, Poland*
[2]*Institute of Botany, Jagiellonian University, Kopernika 27, 31-501 Cracow, Poland*
hubert.haranczyk@uj.edu.pl

Abstract: The effect of low temperature on *Umbilicaria aprina* collected from Schirmacher Oasis, East Antarctica, was determined over a wide range of hydration using proton free induction decays, proton nuclear magnetic resonance (NMR) spectra and differential scanning calorimetry methods. The proton NMR line is a superposition of the broad component from the solid matrix of the thallus and a narrower component from the averaged bound water pool. Proton free induction decays may be resolved into three components: a solid component well described by the Abragam function and two exponentially decaying components from water loosely bound and water tightly bound in the thallus. With decreased temperature the loosely bound water pool (freezing water) is transferred to the tightly bound water pool (non-freezing water), and vanishes below -40°C. Bound water freezing and melting temperatures decrease with the decrease of hydration level, suggesting that heterogeneous ice nucleation is responsible for water freezing. The onset of bound water freezing temperature is *c.* 10°C lower than the melting temperature. The *U. aprina* thalli do not reveal the ability to stimulated ice nucleation at higher temperature. Freeze-thaw cycles showed that for $n > 5$ cycles no substantial change occurs in the difference between melting and freezing temperatures.

Received 20 February 2011, accepted 8 October 2011, first published online 30 March 2012

Key words: DSC, foliose lichenized fungi, freezing resistance, lichens, NMR

Introduction

Freezing tolerance of lichens manifests either in their resistance to low temperature or to the length of the low temperature period. Some lichen species may survive the liquid nitrogen temperature (-196°C) regardless of the rate of cooling, e.g. two species of the genus *Umbilicaria* (*U. decussata* (Vill.) Zahlbr. and *U. vellea* (L.) Ach.) survive slow cooling down to -196°C and fast cooling down to -78°C, or to -50°C (Kappen 1993). The prolonged frozen storage (3.5 years at -60°C) of *Alectoria ochroleuca* (Hoffm.) Massal. does not change its basic photosynthetic and respiratory responses after 12 hours incubation at an elevated temperature (Larson 1978), and *Cladonia foliacea* (Huds.) Willd. (= *Cladonia alcicornis*) recovers its photosynthetic activity after prolonged freezing (96 and 110 weeks at -15°C) (Lange 1966).

Although in *C. foliacea* the photosynthetic activity was detected at -24°C in laboratory conditions (Lange 1965), the lowest temperature (-17°C) for CO_2 exchange rates in the natural habitat (Cape Geology, Antarctica) was recorded for *Umbilicaria aprina* Nyl. thalli. The dark respiration of *U. aprina* significantly decreased at -7°C and finally ceased at -11°C (Schroeter *et al*. 1994). Light maximum value of net photosynthesis declined with temperature in two steps: i) rapidly, between -1°C and -9°C to about 10% of the rate at +1°C, and then ii) more slowly, to very low rates at -17°C. They suggested that a two-step mechanism of net photosynthesis decline with decreasing temperature might be the result of increase of CO_2 diffusion resistance, possibly by the ice nucleation activity (INA), which occurs in water saturated thalli of *Umbilicaria aprina* at -5.4°C (Schroeter & Scheidegger 1995).

Many lichen species reveal biological INA in thallus liquid extracts at temperatures much higher than the low temperature limit of their photosynthetic activity (Nash *et al*. 1987, Kieft 1988, Kieft & Ahmadjian 1989, Kieft & Ruscetti 1990, Schroeter & Scheidegger 1995). The stimulation of ice crystallite growths in extracellular spaces and/or guts is also one of the effective strategies used by some arthropods to deal with extremely low temperatures (Zachariassen 1989, Block *et al*. 1993, Worland *et al*. 1993, Block 1995).

The effectiveness of photosynthetic activity of *U. aprina* far below 0°C focused our attention on the bound water behaviour at temperatures as low as -65°C, and the thermal immobilization of various water fractions differentiated by the proximity to the thallus surfaces. As the mild dehydration of intracellular space (Harańczyk *et al*. 2000a, 2000b) (often accompanied by the stimulated ice nucleation in extracellular spaces (Schroeter & Scheidegger 1995, Harańczyk *et al*. 2003a, 2003b)) is one of the ways to deal with freezing, the observation of thermal behaviour of water bound in thalli, dehydrated to very low water level, is expected to provide additional insight into this very interesting survival mechanism.

We applied techniques involving hydration kinetics, sorption isotherm, proton nuclear magnetic resonance (NMR)

high power relaxometry, proton NMR spectra, and differential scanning calorimetry (DSC) to study bound water freezing in the lichen *Umbilicaria aprina*.

Materials and methods

Sampling was carried out in Schirmacher Oasis, Dronning Maud Land, in the summer 2003–04, during the 23rd Indian Antarctic Expedition. *Umbilicaria aprina* thalli were collected from temporary streams flowing from melting glaciers. In such an untypical habitat lichens grow on boulders and pebbles immersed in water during the short summer period, and are covered by ice in the winter.

Air-dry thalli were stored at $p/p_0 \approx 40\%$ and at room temperature with the hydration level $\Delta m/m_0 = 0.096 \pm 0.010$, where m_0 is the dry mass of the sample, and Δm is mass of water taken up.

Before hydration, air-dry thalli were incubated for 164 hours over silica gel ($p/p_0 = 0\%$), dehydrating to the hydration level of $\Delta m/m_0 = 0.048 \pm 0.004$, then pieces were placed in NMR tubes. The samples to be used for DSC scans were hydrated prior to sealing in DSC capsules.

The samples were hydrated from the gaseous phase over the water surface ($p/p_0 = 100\%$) for t = 4.5 h ($\Delta m/m_0 = 0.125 \pm 0.006$), for 22.5 h ($\Delta m/m_0 = 0.173 \pm 0.010$), for 37 h ($\Delta m/m_0 = 0.213 \pm 0.008$), and for 55.5 h ($\Delta m/m_0 = 0.332 \pm 0.008$).

The vitality tests performed using methylene blue staining showed that no less than 68 ± 5% photobiont cells were alive either in thalli samples which had been used in NMR or in those after 21 days in the capsules used for DSC courses. After completing the temperature courses, the dry mass of the thallus was determined after heating at 70°C for 72 h. Higher temperatures were not used as they may cause the decomposition of some organic constituents of the thallus (Gaff 1977).

Proton free induction decays (FIDs) were recorded on WNS HB-65 high power relaxometer (Waterloo NMR Spectrometers, St Agatha, Ontario, Canada). The resonance frequency was 30 MHz (at $B_0 = 0.7$ T), the transmitter power was 400 W, the pulse length $\pi/2 = 1.4 - 1.5$ μs. The high power of the pulse allowed us to observe the total proton signal. FIDs were acquired using a Compuscope 2000 card in an IBM clone, controlling the spectrometer, and averaged over 2000 accumulations. Repetition time was 2.003 s. The temperature was varied between 25°C and -60°C and was stabilized in a gaseous nitrogen stream.

Proton spectra were acquired with a Bruker Avance III spectrometer (Bruker Biospin), designed for solids, operating at the resonance frequency 300 MHz (at $B_0 = 7$ T), with the transmitter power used equal to 400 W. The pulse length was $\pi/2 = 1.5$ μs, dead time was 7.5 μs, and repetition time was 2 s.

The data obtained were analysed using the FID analysing procedure of a two-dimensional (in time domain) NMR signal-analysing program CracSpin written at the Jagiellonian University, Cracow (Węglarz & Harańczyk 2000).

Differential scanning calorimetry scans were performed in Perkin Elmer DSC 8000 calorimeter using 30 μl aluminum

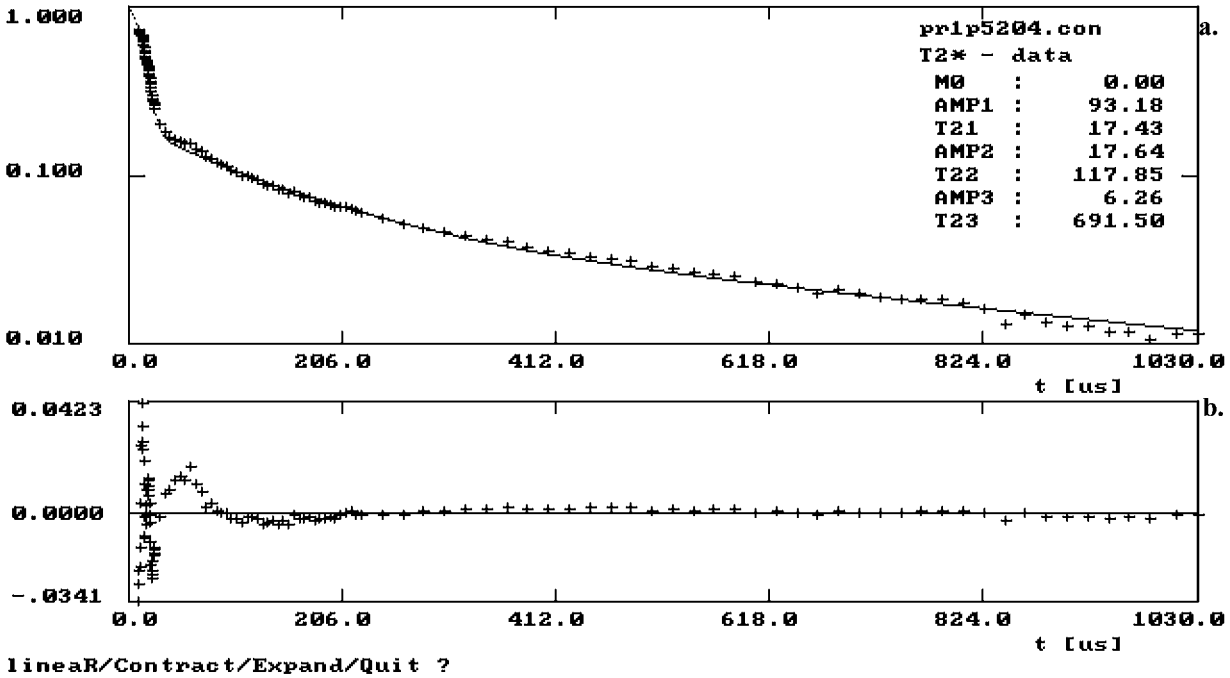

Fig. 1. a. Proton free induction decay recorded for *Umbilicaria aprina* Nyl. thalli at 30 MHz, with the pulse length $\pi/2 = 1.4$ μs at the temperature t = 24°C. The relative mass increase was $\Delta m/m_0 = 0.097$. **b.** The residual function calculated as the difference between the fitted and recorded values of the FID signal, which for any recorded point does not exceed 4.3%.

https://doi.org/10.1017/S0954102012000041 Published online by Cambridge University Press

pans. The calorimeter was calibrated by means of the melting points of indium and water. The mass of the sample used was *c.* 8 mg. Differential scanning calorimetry curves were recorded while cooling from room temperature down to -70°C, followed by heating of the samples, returning to the initial temperature. The heating/cooling rates were varied between 0.1 and 20°C min^{-1}. Since the peak onset temperature was almost independent of the rates tested, a rate of 20°C min^{-1} was used. Onset and peak temperatures as well as transition enthalpies have been calculated by Perkin Elmer software.

Results

Proton free induction decays

Figure 1 shows the proton FID for *Umbilicaria aprina* hydrated to $\Delta m/m_0 = 0.097$. The FID is composed of a solid component and two exponential components from the protons of thallus liquids. The solid signal, with the amplitude S, deriving from protons of the solid matrix of the thallus may be fitted either by the Gaussian (Eq. (1a)) or Abragam (Eq. (1b)) function (Abragam 1961). The exponential components are interpreted as coming from protons of water tightly or loosely bound in the thallus with the amplitudes equal to L_1 and L_2, respectively (Harańczyk *et al.* 2009a).

$$FID(t) = S \cdot \exp\left(-\left(\frac{t}{T^*_{2S}}\right)^2\right) + L_1 \cdot \exp\left(-\frac{t}{T^*_{2L_1}}\right) + L_2 \cdot \exp\left(-\frac{t}{T^*_{2L_2}}\right). \quad (1a)$$

$$FID(t) = S \cdot \exp\left(-\left(\frac{t}{T^*_{2S}}\right)^2\right) \frac{\sin(at)}{at} + L_1 \cdot \exp\left(-\frac{t}{T^*_{2L_1}}\right) + L_2 \cdot \exp\left(-\frac{t}{T^*_{2L_2}}\right). \quad (1b)$$

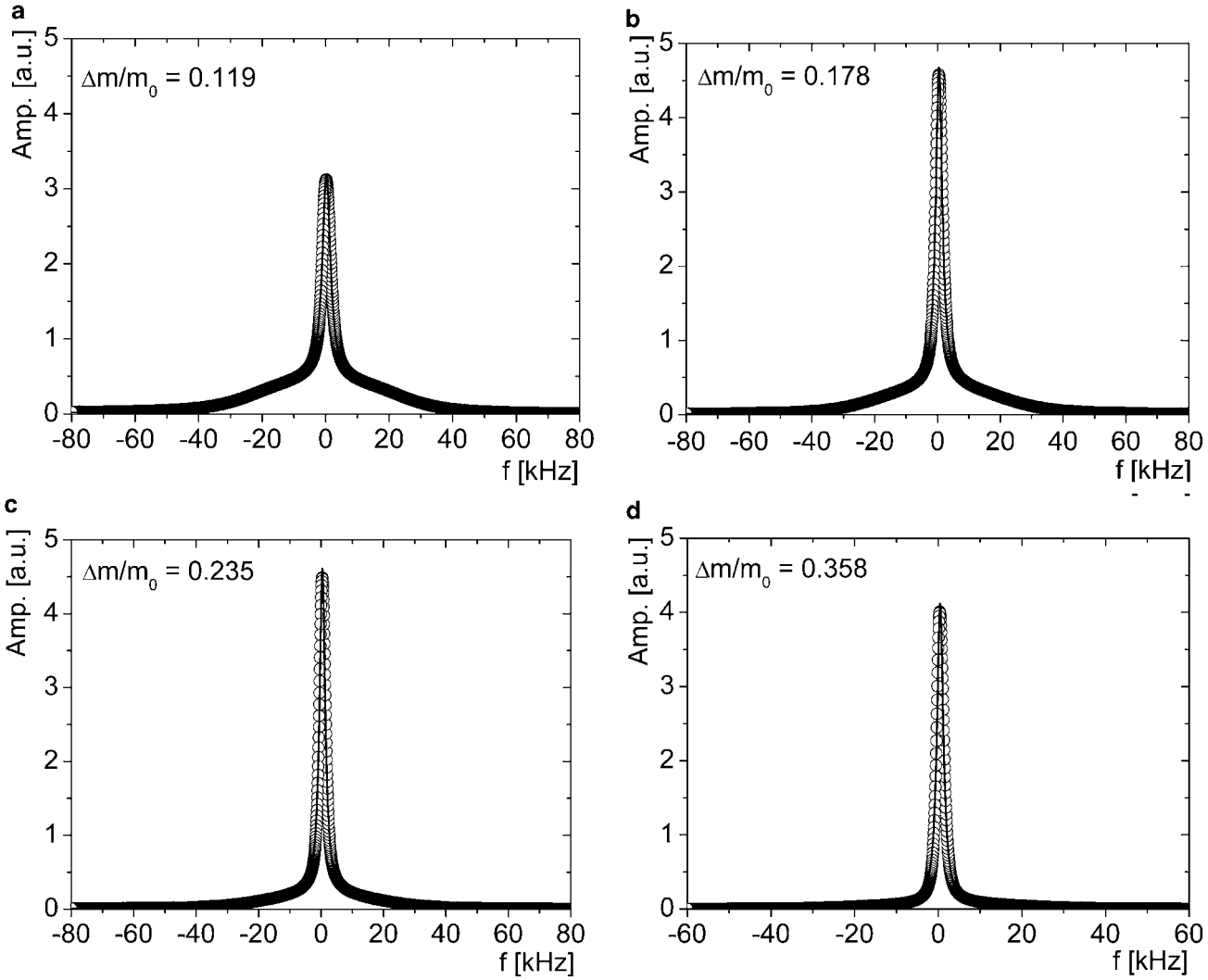

Fig. 2. Proton spectra detected for *Umbilicaria aprina* Nyl. thalli at 300 MHz, with the pulse length $\pi/2 = 1.5$ μs at the temperature t = 24°C. The relative mass increase was **a.** $\Delta m/m_0 = 0.119$, **b.** $\Delta m/m_0 = 0.178$, **c.** $\Delta m/m_0 = 0.235$, and **d.** $\Delta m/m_0 = 0.358$.

https://doi.org/10.1017/S0954102012000041 Published online by Cambridge University Press

Table I. The parameters of ^{1}H-NMR spectra recorded for *Umbilicaria aprina* Nyl. thalli at temperature t = 24°C. The samples were hydrated to $\Delta m/m_0$; peak position are υ_G and υ_L for Gaussian and for Lorentzian line components respectively; line half-widths are $\Delta\upsilon_G$ and $\Delta\upsilon_L$ for Gaussian and Lorentzian line components, respectively; L/S* is the ratio of the area under the liquid line to the area under the solid line; L/S is the ratio of the liquid signal amplitude to solid amplitude, recorded in time domain (FID). Similar hydration levels were used in these two sets of experiments. The peak positions were scaled to the resonance frequency, $\upsilon_0 = 300131000.0$ Hz.

$\Delta m/m_0$	υ_G (Hz)	$\Delta\upsilon_G$ (Hz)	υ_L (Hz)	$\Delta\upsilon_L$ (Hz)	L/S*	L/S
0.119	-(440 ± 43)	39090 ± 120	241.8 ± 2.0	3047.2 ± 7.2	0.604 ± 0.020	0.554 ± 0.014
0.178	1586 ± 68	37450 ± 190	465.5 ± 1.4	2521.6 ± 5.0	1.086 ± 0.006	1.181 ± 0.025
0.235	580 ± 140	37280 ± 390	426.4 ± 1.3	2184.2 ± 4.5	1.980 ± 0.017	1.599 ± 0.018
0.358	7720 ± 830	43100 ± 2200	447.9 ± 1.5	1825.1 ± 5.0	5.88 ± 0.13	1.896 ± 0.039

T^*_{2S} is the transverse proton relaxation time of the solid component taken as the 1/e-value of Gaussian solid signal, and $T^*_{2L_1}$ and $T^*_{2L_2}$ are the transverse proton relaxation times of the liquid-like magnetization components L_1 and L_2, respectively.

The relaxation time T^*_{2S} for the Gaussian component does not vary much with thallus hydration level (Harańczyk *et al.* 2008), suggesting that the structure and molecular dynamics of the thallus solid matrix is hardly modified by the hydration process. Thus, the solid signal amplitude, S, may be used as a reference amplitude to scale the amplitudes of liquid components.

The L_2 signal comes from water loosely bound on thallus surface and for higher hydration level from free water fraction. The $T^*_{2L_2} \approx 510\,\mu$s is shortened by B_0 inhomogeneities, according to Timur (1969).

$$1/T^*_2 = 1/T_2 + \gamma\Delta B_0/2, \qquad (2)$$

where T_2 is spin-spin relaxation time, γ is gyromagnetic ratio, and ΔB_0 is a change of magnetic field B_0 within the sample. The solid components and the short exponential components are negligibly affected by the B_0 inhomogeneities, but T_2 for the L_2 component, associated with loosely bound water pools (e.g. extra- and intramolecular loosely bound water fractions) is much more shortened by ΔB_0 (Eq. (2)).

Proton NMR spectra

Figure 2 shows proton NMR spectra recorded at 24°C for *U. aprina* thallus at various hydration levels. The line is composed of the broad solid component successfully fitted by the Gaussian function and the narrow component coming from water bound in *U. aprina* thallus. Gaussian approximation resembles the 'hat-like' function which is the Fourier transformation of Abragam function detected in time domain for FIDs (Derbyshire *et al*. 2004).

Proton magnetic resonance spectra recorded for the pulse with the power sufficient to detect solid and liquid signal components for *U. aprina* thalli are the superpositions of the solid component, well fitted by a Gaussian function, and the liquid component fitted by Lorentzian function:

$$A(\upsilon) = A_S/\Delta\upsilon_G\cdot\sqrt{\pi}/2\,\exp(-2(\upsilon - \upsilon_G/\Delta\upsilon_G)^2) + 2A_L/\pi(\Delta\upsilon_L/4(\upsilon - \upsilon_L)^2 + \Delta\upsilon_L{}^2), \qquad (3)$$

where $\Delta\upsilon_G$ and $\Delta\upsilon_L$ are the half-widths for the Gaussian and Lorentzian components of the NMR line, respectively, υ_G and υ_L are Gaussian and Lorenztian peak positions, respectively, and finally A_S and A_L are the amplitudes of the Gaussian and Lorentzian peaks, respectively.

Table I gives the parameters obtained by fitting Eq. (3) to the spectra. The half-width of the solid Gaussian line component increased from $\Delta\upsilon_G = 37$ kHz up to 43 kHz, with hydration level increase from $\Delta m/m_0 = 0.119$ up to 0.358, whereas for the liquid component $\Delta\upsilon_L$ increased from 1.8 kHz to 3.0 kHz for the same change in hydration level. The liquid to solid ratios, L/S, obtained in the time domain are similar to those obtained in the frequency domain. An exception is noted for the spectrum recorded for the thallus hydrated to $\Delta m/m_0 = 0.358$, for which the area under the solid peak is decreased. This may be an effect of a ripple form of baseline caused by phase drift.

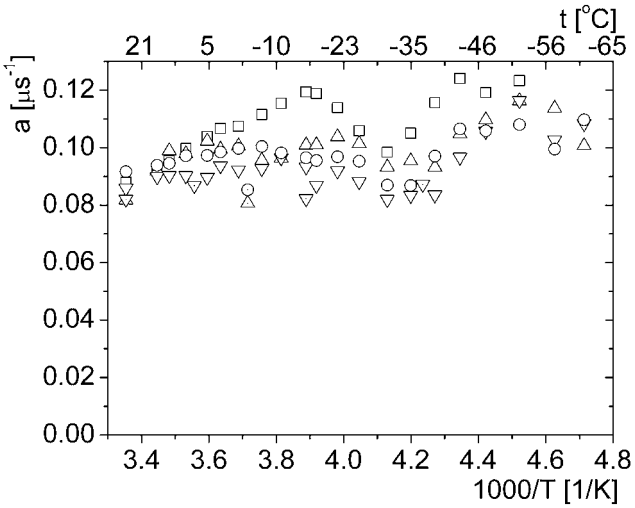

Fig. 3. The temperature dependence of the parameter a for Abragam function fitted to solid component signal (thallus solid matrix line widths) calculated for *Umbilicaria aprina* Nyl. thalli with various hydration levels: $\Delta m/m_0 = 0.125$ (squares), $\Delta m/m_0 = 0.173$ (upward triangles), 0.213 (downward triangles), and 0.332 (circles). Open symbols = cooling down, dotted symbols = heating up.

https://doi.org/10.1017/S0954102012000041 Published online by Cambridge University Press

The relaxation time for the solid (Gaussian) component, T^*_{2G}, may be calculated from

$$T^*_{2G} = \sqrt{2}/\pi.\Delta\upsilon_G, \quad (4)$$

whereas the relaxation time for the liquid component, T^*_{2L}, from

$$T^*_{2L} = 1/\pi.\Delta\upsilon_L. \quad (5)$$

The values of relaxation times calculated from the parameters fitted for proton spectra (Eqs (4) & (5)), in the frequency-domain experiment, agree with those fitted from proton FIDs, in the time-domain measurement. If the relaxation times are defined for the half-intensity value of the line, for the solid component they vary from $T^*_{2G} = 10$ μs up to 12 μs, whereas for liquid component $T^*_{2L} = 104 - 174$ μs. If the relaxation times are recalculated for 1/e value, for the solid component they vary from 14.5 μs up to 17 μs, which is close to the values obtained in time-domain experiment. The difference between the relaxation times for the liquid component, T^*_{2L}, is greater than that for the solid component and is caused by higher value of ΔB_0 (Eq. (2)) in the frequency-domain experimental setup.

Temperature dependency of proton FID parameters

Figure 3 shows the temperature dependencies of the parameter *a* for the *U. aprina* thalli at the hydration level varied from $\Delta m/m_0 = 0.125$ up to 0.332. For given temperature the value of *a* parameter depends on hydration level of thallus only weakly, suggesting that for hydration

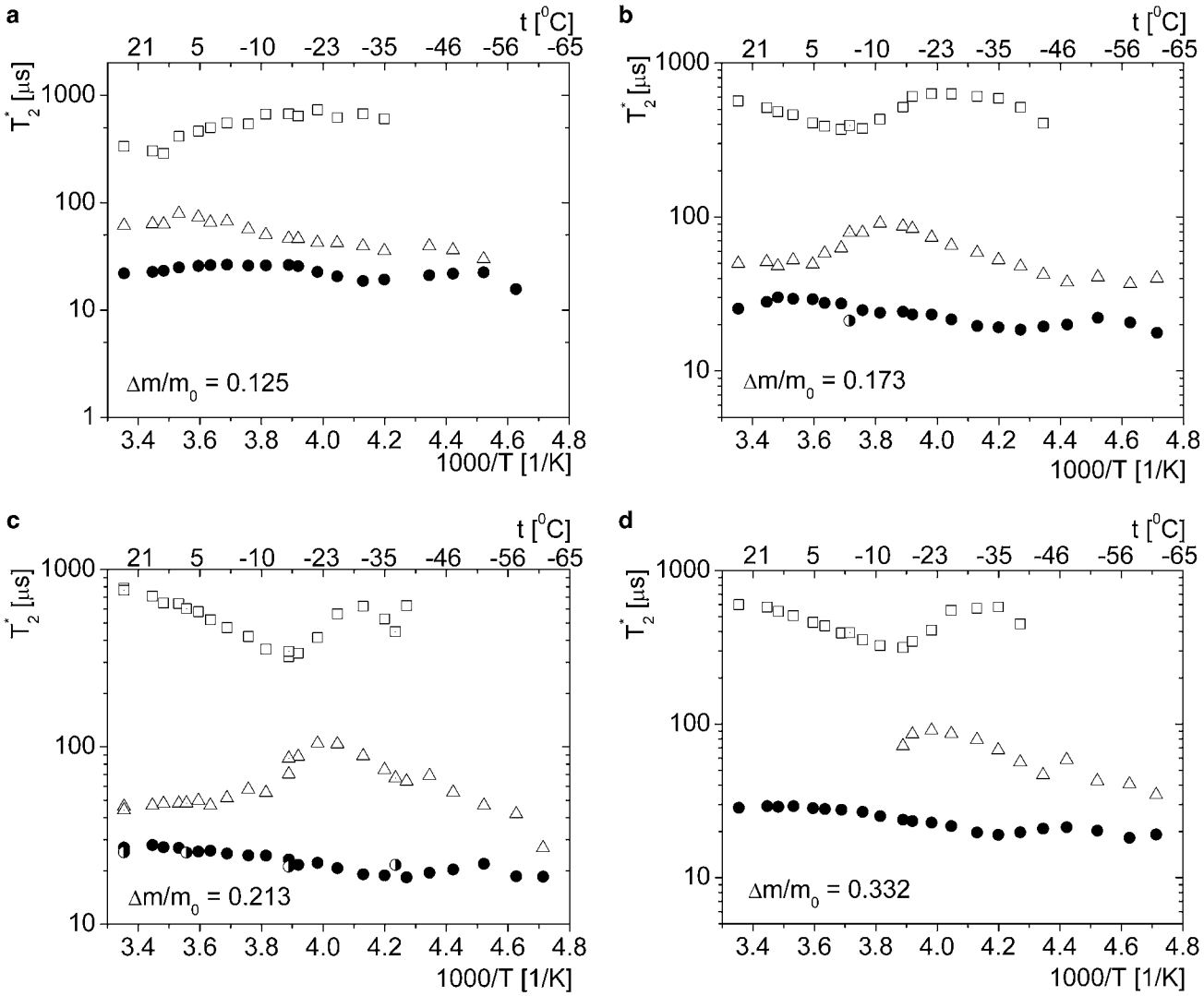

Fig. 4. a–d. The temperature dependence of proton FID relaxation times for *Umbilicaria aprina* Nyl. thalli hydrated to $\Delta m/m_0 = 0.125$, 0.173, 0.213, and to $\Delta m/m_0 = 0.332$, respectively. Solid Gaussian component (S) = closed circles, tightly bound water component (L_1) = open triangles, and loosely bound water fraction (L_2) = open squares. For temperatures below -40°C the loosely bound water signal component was not detected. Dotted symbols for heating up of the samples.

https://doi.org/10.1017/S0954102012000041 Published online by Cambridge University Press

levels between $\Delta m/m_0 = 0.125$ and 0.332 the hydration process does not much modify the solid matrix of thallus. In the temperature range from 25°C to -35°C the solid component line widths (proportional to the value of a) remains unchanged, which indicates the absence of phase transitions. For the temperatures below -35°C the solid component NMR line becomes broader, which means the immobilization of some protons of the thallus solid matrix. The line widths increase up to $\Delta\nu_G = 35$ kHz.

Figure 4a–d presents the Arrhenius plots of the proton spin-spin relaxation times for all FID signal components detected in *U. aprina* thalli hydrated to $\Delta m/m_0 = 0.125$, 0.173, 0.213, and $\Delta m/m_0 = 0.332$, respectively. For the temperatures higher than -40°C the liquid part of FID signal is fitted by two exponentials L_1 and L_2 coming from water tightly bound and loosely bound to the surfaces of the thallus, respectively. For the sample hydrated to the highest hydration level ($\Delta m/m_0 = 0.332$) and for the temperatures above -11°C only one exponential component L_2, coming from loosely bound water, was detected. As the signal of L_2 decreased with the decreasing temperature, below -11°C only the smaller amplitude, the tightly bound water component, L_1, was fitted. Below -40°C, for all hydration levels investigated, the loosely bound water component, L_2, was not detected, leaving only the exponential FID component of tightly bound water.

For the solid signal component the relaxation time, T_{2S}^*, does not vary much with the temperature (Fig. 3),

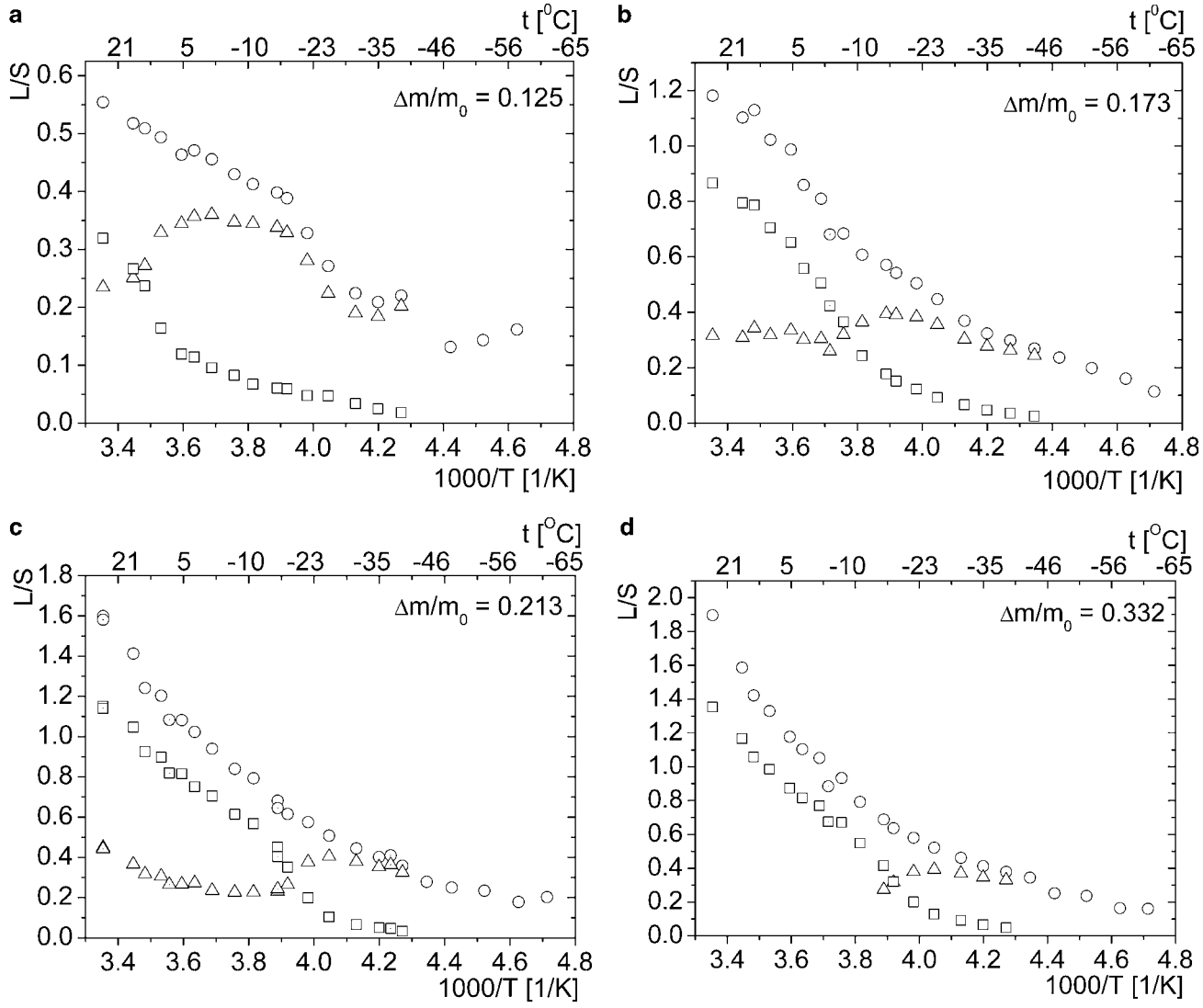

Fig. 5. The total liquid signal, $(L_1+L_2)/S$ (open circles), L_1/S (open triangles), and L_2/S (open squares), temperature dependency for *Umbilicaria aprina* Nyl. thalli hydrated to **a.** $\Delta m/m_0 = 0.125$, **b.** $\Delta m/m_0 = 0.173$, **c.** $\Delta m/m_0 = 0.213$, and **d.** $\Delta m/m_0 = 0.332$, respectively. Dotted symbols for heating courses.

https://doi.org/10.1017/S0954102012000041 Published online by Cambridge University Press

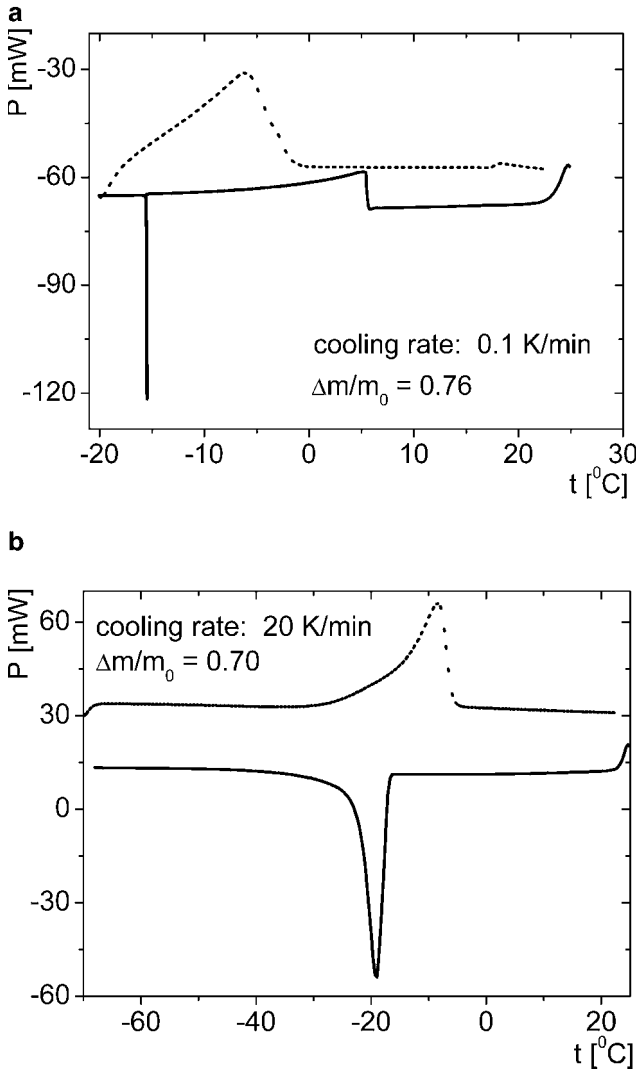

Fig. 6. Calorimetric scans of freezing (peak down) and melting (peak up) of water bound in *Umbilicaria aprina* Nyl. thalli recorded at two different rates, **a.** 0.1°C min^{-1}, and **b.** 20°C min^{-1}. The hydration level of the thallus was $\Delta m/m_0 = 0.76$, and 0.70, respectively.

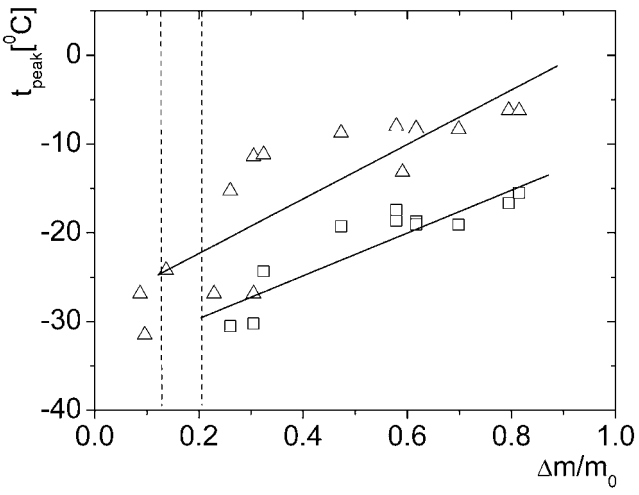

Fig. 7. The bound water freezing (open squares) and melting (open triangles) onset temperatures recorded for *Umbilicaria aprina* Nyl. thalli as a function of the relative mass increase $\Delta m/m_0$.

suggesting that the structure of the solid matrix of the thallus is not appreciably modified by the hydration process (Harańczyk *et al.* 2008). Thus we used solid signal amplitude, S, to scale the amplitudes of liquid components for every given temperature.

The temperature dependence of total liquid signal, expressed in the units of solid signal, $(L_1 + L_2)/S$, is shown in Fig. 5 (open circles). The amplitude of liquid signal decreases continuously with temperature decrease. The co-operative bound water freezing should manifest as the discrete decrease in the proton liquid signal, which was not observed. With decreasing temperature the contribution of the tightly bound water signal, L_1, increases at the expense of the loosely bound water signal L_2 and below -40°C the L_2 component is no longer detected. The change occurs smoothly over broad temperature range.

DSC temperature scans

The differential scanning calorimetry reveals bound water freezing in *U. aprina* thalli, at a temperature which did not change with the cooling speed being varied from 0.1°C min^{-1} up to 20°C min^{-1}. The onset temperatures were -15.68°C and -15.52°C, for thalli hydrated to $\Delta m/m_0 = 0.70$, and to 0.76, respectively (see Fig. 6a & b). Thus, all other temperature trials were performed with the cooling/heating rate equal to 20°C min^{-1}.

For *U. aprina* thalli the onset temperatures for melting and for freezing (Fig. 7) depend linearly on the thallus hydration level, according to the formulae

$$t_m[^\circ C] = (30.7 \pm 5.4)\cdot\Delta m/m_0 - (28.5 \pm 20.6), \quad (6a)$$

$$t_f[^\circ C] = (24.1 \pm 4.2)\cdot\Delta m/m_0 - (34.5 \pm 2.4). \quad (6b)$$

The linear dependence of water melting temperature on hydration level correlates the freezing onset with the sizes of water compartments in porous material (Harańczyk 2003, and references therein). This means that heterogeneous ice nucleation is responsible for bound water freezing in *U. aprina* thallus.

The estimated bound water melting temperature for zero-hydration of the thallus equals $t_m = -(28.5 \pm 2.6)$°C, whereas the freezing temperature equals $t_f = -(24.1 \pm 4.2)$°C. For melting onset and for freezing onset the estimated temperatures are substantially higher than the singularity temperature of water (Angell 1982).

https://doi.org/10.1017/S0954102012000041 Published online by Cambridge University Press

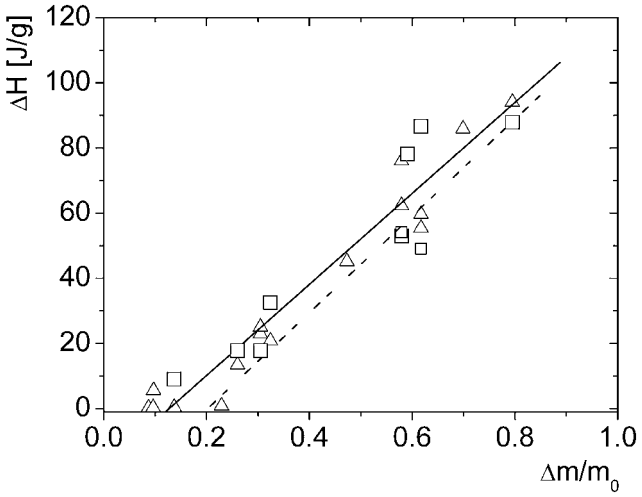

Fig. 8. The transition enthalpy for bound water freezing (open squares) and melting (open triangles) for *Umbilicaria aprina* Nyl. thalli as a function of the relative mass increase $\Delta m/m_0$.

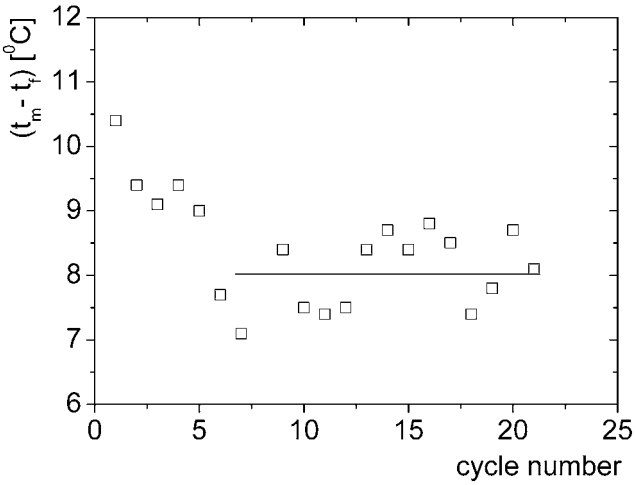

Fig. 10. The difference between bound water melting and water freezing onset temperatures, $t_m - t_f$, detected as a function of freeze-thawing cycles for *Umbilicaria aprina* Nyl. thalli hydrated to $\Delta m/m_0 = 0.744$.

The transition enthalpy, ΔH_f and ΔH_m, of freezing and of melting (see Fig. 8), respectively, linearly depends on hydration level of *U. aprina* thallus (Eq. (7a) & (7b)):

$$\Delta H_f(J/g) = (148.5 \pm 13.4).\Delta m/m_0 - (30.0 \pm 7.2), \quad (7a)$$

$$\Delta H_m(J/g) = (139.7 \pm 3.8).\Delta m/m_0 - (17.8 \pm 3.8). \quad (7b)$$

In the linear approximation, the hydration level for which the transition enthalpy, ΔH, reaches zero with decreasing hydration level equals $\Delta m/m_0 = 0.202 \pm 0.050$ for cooling (for freezing), and $\Delta m/m_0 = 0.127 \pm 0.027$ for heating of the sample (for melting). This value approximates the minimal hydration level at which the co-operative freezing of bound water occurs.

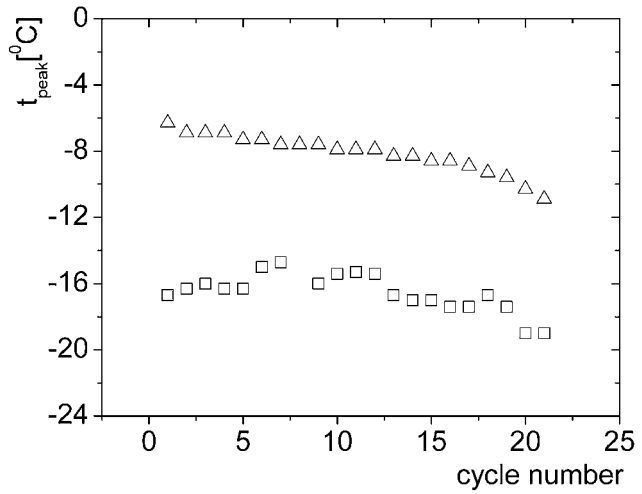

Fig. 9. The freezing (open squares) and melting (open triangles) peak temperatures recorded as a function of freeze-thawing cycles for *Umbilicaria aprina* Nyl. thalli hydrated to $\Delta m/m_0 = 0.744$.

Freeze-thaw cycles

Calorimetric freeze-thaw scans were performed between room temperature and -70°C. The number of cycles was $n = 22$. The melting temperature, t_m, slightly decreases with the number of the cycle, whereas a change in freezing temperature, t_f, is not seen (Fig. 9). The temperature difference between bound water melting and bound water freezing onsets, $t_m - t_f$, decreases for $n \leq 5$ cycles, and remain constant ($t_m - t_f = (8.0 \pm 0.2)$) for $n > 5$ cycles (Fig. 10). This suggests that the structural changes in the thallus appear only if the temperature is periodically changed not too many times. This may reflect the adaptation of thallus to subsequent freeze-thaw cycles.

Discussion

In many biological microheterogeneous systems, e.g. in dentine, dental enamel, shells of molluscs, bark and bast (e.g. Harańczyk *et al*. 1998, and references therein), the solid signal is usually nearly Gaussian in form, with the relaxation time, T_{2S}^*, close to the value obtained by us for *U. aprina* thallus. This suggests similar distribution of local magnetic fields in organic matter (Pintar 1991). The 'beat pattern' observed in the solid part of FID signal suggests that the solid component contribution may be successfully fitted by an Abragam function (Derbyshire *et al*. 2004). The parameter a in Abragam function yields the half-widths of the NMR line solid component as: $\Delta\omega = 2.a$ ($\Delta\upsilon_G = a/\pi$). The 'beat pattern' in FID function manifests itself in frequency domain as a 'hat-like' form of the solid line

https://doi.org/10.1017/S0954102012000041 Published online by Cambridge University Press

component (Derbyshire *et al*. 2004). The observed water fractions are differentiated by their mobility and, thus, by their binding and/or proximity to the thallus surfaces, which means that intracellular water as well as extracellular water fraction usually contributes to both these water fractions. In proton FID the $T^{*}_{2L_1} \approx 60\,\mu s$ of the L_1 component recorded for *U. aprina* is close to that recorded for tightly bound water of lichen thalli (Harańczyk *et al*. 2000a, 2006a, 2009a), as well as of biological macromolecules (Harańczyk *et al*. 2010) or photosynthetic membranes (Harańczyk *et al*. 2006b, 2009b, 2009c).

The upper limits of hydration levels *in situ* for lichens of the genus *Umbilicaria* significantly exceed the hydration level obtained by us for *U. aprina* hydrated from gaseous phase, e.g. for *Umbilicaria spodochroa* (Hoffm.) DC. in Lam. & DC. $\Delta m/m_0$ varies between 1.0 and 5.0 (Kappen *et al*. 1996a), for *U. cinereorufescens* (Schaer.) Frey. $\Delta m/m_0 = 1.55$, and for *U. polyrrhiza* (L.) Fr. $\Delta m/m_0 = 3.10$ (Valladares *et al*. 1998). For *U. decussata* the optimal net photosynthesis is recorded at a lower hydration level of $\Delta m/m_0 = 1.0$, for *U. aprina* at $\Delta m/m_0 = 1.2$, for *Usnea antarctica* Du Rietz and for *Usnea sphacelata* R. Br. at $\Delta m/m_0 = 0.85$ (Kappen & Breuer 1991), which are values closer to those used in our experiments.

Polyhydric alcohols and simple sugars may act as cryoprotectants for Antarctic arthropods and for a variety of plants (Kaurin *et al*. 1981, Block & Sømme 1983, Duman 1984). Polyol content in Antarctic lichen thalli, as identified by ^{13}C-NMR, varied between $17\,mg\,g^{-1}$ for *Candelariella flava* (Dodge & Baker) Castello & Nimis (= *Candelariella hallettenensis* (Murray) Ørsted) and $65\,mg\,g^{-1}$ for *Usnea antarctica*, with dominating contributions from arabitol, mannitol and ribitol, whereas sorbitol was not detected. Sugar content was approximately one order of magnitude smaller than the content of polyols (Chapman *et al*. 1994). The polyols (ribitol, mannitol, arabitol), as essential metabolites, were present in thalli of *Evernia esorediosa* (Müll. Arg.) Du Rietz, in *Ramalina subbreviuscula* Asah., and in *Ramalina sublitoralis* Ash., at constant level (up to 3.4% w/w of arabitol in *Ramalina subbreviuscula*) under field conditions. Glucose and fructose were not found, and the significant content of monosugars was only forced by external osmotic conditions (Hamada *et al*. 1994). For *Umbilicaria decussata* the carbohydrate level changes only slightly with the thallus hydration level (Melick & Seppelt 1994).

The cryoprotective action of polyols is based on blocking the formation of ice crystallites by steric mismatch of hydrogen bonds which may be formed between them and water. Although the overall concentration of polyols detected in the thallus is not sufficient to promote a significant decrease of freezing point of cellular aqueous medium, if polyols are localized mainly in intracellular spaces, they may contribute to the freezing protection mechanism in lichens.

The observed transformation of bulk water to less mobile fraction during the cooling of *Umbilicaria aprina* thalli suggests that the steric mismatch is not the only effect responsible for the freezing resistance of lichens. If the freezing protection mechanism was based on steric effects alone, drastic changes in motional properties of bound water should not be observed. The immobilization of water suggests the presence of an active mechanism, based on formation of a long range molecular network, increases the area of liquid-solid interface, thus increasing the tightly bound water amount, e.g. a gel-like structure from liquid substances formation.

The mechanism of water transfer from loosely bound, freezing fraction to tightly bound, non-freezing fraction occurring with decreased temperature was observed in fruticose lichens, in *Cladonia mitis* Sandst., *Himantormia lugubris* (Hue) I. M. Lamb, and *Usnea aurantiaco-atra* (Jacq.) Bory (Harańczyk *et al*. 2000a, 2003b). We present here the first observation of loosely bound to tightly bound water transfer in a lichen with a foliose thallus.

The solid component immobilization detected as increase in parameter *a* of Abragam function describing the solid line component in time domain (FID), may be connected with the discontinuous increase in activation energy at -30°C, seen on the Arrhenius plot for proton spin-lattice relaxation time T_1 in dry *Cladonia mitis* thalli (Harańczyk *et al*. 2000b). The phase transition in *Cladonia mitis* was not accompanied by the co-operative bound water immobilization (freezing), which was also observed by us in *U. aprina*. Although there is no evidence on phase transitions in the lichen thallus, there are some reports on phase transitions from liquid crystalline to gel phase occurring for some fraction of lipids, e.g. lipid liposomes, formed from the extracted spinach lipids at -30°C and at -40°C (Jensen *et al*. 1981), in tomato chloroplast lipids at -29°C (Graham & Patterson 1982), and in soya lecithin between -20°C and -30°C (Quinn & Williams 1983).

The temperature for freezing of bound water detected in the present study (Fig. 7) for *U. aprina* thallus was far below the value -6°C reported by Schroeter *et al*. (1994). Although they used differential thermal analysis (DTA) which is a more sensitive method, it does not provide quantitative parameters for thermal peaks, which DSC does. We suggest that the difference cannot be caused by the method of the measurement. The dependence of the bound water freezing temperature on hydration suggests a different molecular mechanism for the freezing process. The linear dependency of the freezing temperature of supercooled water on hydration is characteristic for heterogeneous nucleation of ice crystallites (Angell 1982, and references therein). In *U. aprina* thallus the freezing temperature dependence on hydration level is approximately linear, reflecting the real size distribution of water micro-compartments filled with increased water content. However, this observation indicates that the mechanism of stimulated

https://doi.org/10.1017/S0954102012000041 Published online by Cambridge University Press

ice nucleation did not act in *U. aprina* harvested from glacial streams in Schirmacher Oasis. This observation suggests that *U. aprina* may change its survival strategy from freezing tolerance to freezing avoidance.

Insects are able to fundamentally change their survival strategy (Block 1995). Larvae of two beetle species, *Cucujus clavipes* Fabr., and *Dendroides canadensis* Latr., populating the same sites in northern Indiana, switched from freeze tolerance to freeze avoidance in a relatively short period of time. The change in strategy was induced by a sequence of mild winters and probably occurred between the winters 1979–80 and 1980–81 when ice nucleating agents were lost (Duman 1984, Horwath & Duman 1984). However, the molecular mechanism triggering the change of the survival strategy from freezing tolerance to freezing avoidance is not yet known either for insects or for lichens.

Acknowledgements

The research was carried out with the equipment purchased thanks to the financial support of the European Regional Development Fund in the framework of the Polish Innovation Economy Operational Program (contract no. POIG.02.01.00-12-023/08). We are thankful to colleagues from Maitri Station and participants of the 23rd Indian Antarctic Expedition for their help during the field studies. We would like to thank the reviewers for their comments and suggested improvements.

References

Abragam, A. 1961. *The principles of nuclear magnetism*. Oxford: Clarendon Press, 597 pp.

Angell, C.A. 1982. Supercooled water. *In* Franks, F., *ed. Water: a comprehensive treatise*, vol. 7. New York: Plenum Press, 1–81.

Block, W. 1995. Insects and freezing. *Science Progress*, **78**, 349–372.

Block, W. & Sømme, L. 1983. Low temperature adaptations in beetles from the sub-Antarctic island of South Georgia. *Polar Biology*, **2**, 109–114.

Block, W., Grubor-Lajsic, G. & Worland, R. 1993. Cold tolerance of a larval tipuloid from an upland habitat. *Cryo-Letters*, **14**, 185–192.

Chapman, B.E., Roser, D.J. & Seppelt, R.D. 1994. ^{13}C-NMR analysis of Antarctic cryptogam extracts. *Antarctic Science*, **6**, 295–305.

Derbyshire, W., van Den Bosch, M., van Dusschoten, D., MacNaughtan, W., Farhat, I.A., Hemminga, M.A. & Mitchell, J.R. 2004. Fitting of the beat pattern observed in NMR free-induction decay signals of concentrated carbohydrate-water solutions. *Journal of Magnetic Resonance*, **168**, 278–283.

Duman, J.G. 1984. Change in overwintering mechanism of the cucujid beetle *Cucujus clavipes*. *Journal of Insect Physiology*, **30**, 235–239.

Gaff, D.F. 1977. Desiccation tolerant vascular plants of southern Africa. *Oecologia*, **31**, 95–109.

Graham, D. & Patterson, B.D. 1982. Responses of plants to low, non-freezing temperatures: proteins, metabolism and acclimation. *Annual Review of Plant Physiology*, **33**, 347–372.

Hamada, N., Okazaki, K. & Shinozaki, M. 1994. Accumulation of monosaccharides in lichen mycobionts cultured under osmotic conditions. *Bryologist*, **97**, 176–179.

Harańczyk, H. 2003. *On water in extremely dry biological systems*. Kraków: Wydawnictwo Uniwersytetu Jagiellonskiego, 276 pp.

Harańczyk, H., Bacior, M. & Olech, M.A. 2008. Deep dehydration of *Umbilicaria aprina* thalli observed by proton NMR and sorption isotherm. *Antarctic Science*, **20**, 527–535.

Harańczyk, H., Gaździński, S. & Olech, M.A. 1998. The initial stages of lichen hydration as observed by proton magnetic relaxation. *New Phytologist*, **138**, 191–202.

Harańczyk, H., Gaździński, S. & Olech, M.A. 2000a. Freezing protection mechanism in *Cladonia mitis* as observed by proton magnetic relaxation. *Bibliotheca Lichenology*, **75**, 265–274.

Harańczyk, H., Gaździński, S. & Olech, M.A. 2000b. Low temperature effect on the thallus of *Cladonia mitis* as observed by proton spin-lattice relaxation. *Molecular Physics Reports*, **29**, 135–138.

Harańczyk, H., Grandjean, J. & Olech, M.A. 2003a. Freezing of water bound in lichen thallus as observed by ^{1}H NMR. I. Freezing of loosely bound water in *Cladonia mitis* at different hydration levels. *Colloids & Surfaces B: Biointerfaces*, **28**, 239–249.

Harańczyk, H., Leja, A. & Strzałka, K. 2006a. The effect of water accessible paramagnetic ions on subcellular structures formed in developing wheat photosynthetic membranes as observed by NMR and by sorption isotherm. *Acta Physica Polonica*, **A109**, 389–398.

Harańczyk, H., Bacior, M., Jastrzębska, P. & Olech, M.A. 2009a. Deep dehydration of Antarctic lichen *Leptogium puberulum* Hue observed by NMR and sorption isotherm. *Acta Physica Polonica*, **A115**, 516–520.

Harańczyk, H., Czak, J., Nowak, P. & Nizioł, J. 2010. Initial phases of DNA rehydration by NMR and sorption isotherm. *Acta Physica Polonica*, **A117**, 257–262.

Harańczyk, H., Grandjean, J., Olech, M.A. & Michalik, M. 2003b. Freezing of water bound in lichen thallus as observed by ^{1}H NMR. II. Freezing protection mechanisms in a cosmopolitan lichen *Cladonia mitis* and in Antarctic lichen species at different hydration levels. *Colloids & Surfaces B: Biointerfaces*, **28**, 251–260.

Harańczyk, H., Leja, A., Jemioła-Rzemińska, M. & Strzałka, K. 2009c. Maturation processes of photosynthetic membranes observed by proton magnetic relaxation and sorption isotherm. *Acta Physica Polonica*, **A115**, 526–532.

Harańczyk, H., Pietrzyk, A., Leja, A. & Olech, M. 2006b. Bound water structure on the surfaces of *Usnea antarctica* as observed by NMR and sorption isotherm. *Acta Physica Polonica*, **A109**, 411–416.

Harańczyk, H., Bacior, M., Jamróz, J., Jemioła-Rzemińska, M. & Strzałka, K. 2009b. Rehydration of DGDG (digalactosyl diacylglicerol) model membrane lyophilizates observed by NMR and sorption isotherm. *Acta Physica Polonica*, **A115**, 521–525.

Horwath, K.L. & Duman, J.G. 1984. Yearly variations in the overwintering mechanisms of the cold hardy beetle *Dendroides canadensis*. *Physiological Zoology*, **57**, 40–45.

Jensen, M., Heber, U. & Oettmeier, W. 1981. Chloroplast membrane damage during freezing: the lipid phase. *Cryobiology*, **18**, 322–335.

Kappen, L. 1993. Plant activity under snow and ice, with particular reference to lichens. *Arctic*, **46**, 297–302.

Kappen, L. & Breuer, M. 1991. Ecological and physiological investigations in continental Antarctic cryptogams. II. Moisture relations and photosynthesis of lichens near Casey Station, Wilkes Land. *Antarctic Science*, **3**, 273–278.

Kappen, L., Schroeter, B., Hestmark, G. & Winkler, J.B. 1996a. Field measurements of photosynthesis of Umbilicarious lichens in winter. *Botanica Acta*, **109**, 292–298.

Kaurin, A., Juttila, O. & Hansen, J. 1981. Seasonal changes in frost hardiness in cloudberry *Rubus chamaemorus* in relation to carbohydrate content with special reference to sucrose. *Physiologia Plantarum*, **52**, 310–314.

Kieft, T.L. 1988. Ice nucleation activity in lichens. *Applied and Environmental Microbiology*, **54**, 1678–1681.

Kieft, T.L. & Ahmadjian, V. 1989. Biological ice nucleation activity in lichen mycobionts and photobionts. *The Lichenologist*, **21**, 355–362.

Kieft, T.L. & Ruscetti, T. 1990. Characterization of biological ice nuclei from a lichen. *Journal of Bacteriology*, **172**, 3519–3523.

LANGE, O.L. 1965. Der CO_2 Gaswechsel von Flechen bei tiefen Temperaturen. *Planta*, **64**, 1–19.

LANGE, O.L. 1966. CO_2-Gaswechsel der Fleche *Cladonia alcicornis* nach langfristigem Aufenthalt bei tiefen Temperaturen. *Flora*, **156**, 500–502.

LARSON, D.W. 1978. Patterns of lichen photosynthesis and respiration following prolonged frozen storage. *Canadian Journal of Botany*, **56**, 2119–2123.

MELICK, D.R. & SEPPELT, R.D. 1994. The effect of hydration on carbohydrate levels, pigment content and freezing point of *Umbilicaria decussata* at a continental Antarctic locality. *Cryptogram Botany*, **4**, 212–217.

NASH III, T.H., KAPPEN, L., LOESCH, R., LARSON, D.W. & MATTHES-SEARS, U. 1987. Cold resistance of lichens with Trentepohlia- or Trebouxia-photobionts from the North American west coast. *Flora*, **179**, 241–251.

PINTAR, M.M. 1991. Some considerations of the round table subject. *Magnetic Resonance Imaging*, **9**, 753–754.

QUINN, P.J. & WILLIAMS, W.P. 1983. The structural role of lipids in photosynthetic membranes. *Biochimica et Biophysica Acta*, **737**, 223–266.

SCHROETER, B. & SCHEIDEGGER, C.H. 1995. Water relations in lichens at subzero temperatures: structural changes and carbon dioxide exchange in the lichen *Umbilicaria aprina* from continental Antarctica. *New Phytologist*, **131**, 273–285.

SCHROETER, B., GREEN, T.G.A., KAPPEN, L. & SEPPELT, R.D. 1994. Carbon dioxide exchange at subzero temperatures. Field measurements on *Umbilicaria aprina* in Antarctica. *Cryptogam Botany*, **4**, 233–241.

TIMUR, A. 1969. Pulsed nuclear magnetic resonance studies of porosity, movable fluid, and permeability of sandstones. *Journal of Petroleum Technology*, **21**, 775–786.

VALLADARES, F., SANCHO, L.G. & ASCASO, C. 1998. Water storage in the lichen family Umbilicariacae. *Botanica Acta*, **111**, 99–107.

WĘGLARZ, W. & HARAŃCZYK, H. 2000. Two-dimensional analysis of the nuclear relaxation function in the time domain: the program CracSpin. *Journal of Physics D: Applied Physics*, **33**, 1909–1920.

WORLAND, M.R., BLOCK, W. & ROTHERY, P. 1993. Ice nucleation studies of two beetles from sub-Antarctic South Georgia. *Polar Biology*, **13**, 105–112.

ZACHARIASSEN, K.E. 1989. Thermal adaptations to polar environments. *In* MERCER, J.B., *ed. Thermal physiology*. Amsterdam: Elsevier, 23–34.